Small angle X-ray and neutron scattering on cadmium sulfide nanoparticles in silicate glass

Y. V. Kuznetsova[1], A. A. Rempel[1,2], M. Meyer[3], V. Pipich[4], S. Gerth[5], A. Magerl[5]

[1]Institute of Solid State Chemistry, Ural Branch of the Russian Academy of Sciences, 620990 Ekaterinburg, Russia

[2]Ural Federal University, 620002 Ekaterinburg, Russia

[3]Juelich Centre for Neutron Science and Institute for Complex Systems, Forschungszentrum Juelich GmbH, ICS-JCNS, 52425 Juelich, Germany

[4]Research neutron source Heinz Maier-Leibnitz, FRM II, 85747 Garching, Germany

[5]Crystallography and Structural Physics, University of Erlangen-Nuremberg, 91058 Erlangen, Germany

Abstract

Small angle X-ray and neutron scattering on Cd and S doped glass annealed at 600 °C shows after the first 9 h nucleation and growth of spherical CdS nanoparticles with a radius of up to 34±4 Å. Towards 48 h the particle shape has changed into spheroidal with short and long axis of 40±2 and 120±2 Å, respectively. After the nucleation is completed after 24 h, further growth in this amorphous environment is governed by oriented particle attachment mechanism as found for a liquid medium.

Keywords: nanoparticles, quantum dots, CdS, glass, SAS

1. Introduction

Small semiconductor nanoparticles or quantum dots (QDs) have an immense potential for application in fields like optoelectronics [1-7] and biomedicine [8, 9] due to the nonlinear optical properties of these materials [10], the tunable high intensity photoluminescence [11], and a narrow emission line width together with a wide absorption range [12]. When the particles are small their stability in general is fragile due to high excess energy of the surface. This latter fact also results in rapid particle growth in supersaturated conditions by atomic attachment. When low supersaturation is reached at later times, growth may occur through particle attachment or through Ostwald ripening. Hence attempts have been made to stabilize QDs at a specific size and to avoid their agglomeration using polymers or glass matrixes [13-22]. Use of a silicate glass in particular as the QDs matrix appears to be particularly attractive since it is based on a cheap production technology and it resists to chemical and environmental damage [23-25]. Further, as

growth is diffusion controlled and only relevant at elevated temperature the size of the QDs can be easily controlled through a temperature profile, giving specific properties of the material.

In this study cadmium sulfide (CdS) nanoparticles were nucleated and grown thermally in a silicate glass matrix, and small angle X-ray (SAXS) and neutron (SANS) scattering [26-28] have been used to analyze their geometrical properties.

2. Experimental

2.1 Synthesis

The synthesis of nanoparticles embedded in a glass matrix explored in the present experiment is based on commercial technologies developed for the fabrication of color cut-off filters and photochromic glasses [29, 30]. Diffusion controlled growth from a supersaturated solution can be described in terms of three distinct precipitation stages, namely nucleation, normal growth, and competitive growth under specific conditions [15, 31-34]. First, nuclei are formed due to fluctuations in the local concentration of the reactants. Second, these particles grow by diffusion of reactants to the surface of the nuclei. In this stage, the number of particles remains constant, while their size increases. Third, after the Cd and/or S concentration has dropped below a specific level, and larger particles continue to grow while smaller particles dissolve. This final stage is also known as the coarsening or ripening stage, also termed Ostwald ripening.

This complex sequence of processes is driven by the phase transition in a supersaturated solution [15, 29], and the time constant of particle formation is controlled by the diffusion of ions dissolved in the matrix. The material synthesis can be performed in a temperature range $T_{glass} < T < T_{melt}$, where T_{glass} and T_{melt} are the glass transition temperature and the melting temperature, respectively [23, 29, 30].

A glass made from high purity powders with compositions 64 % SiO_2, 13 % ZnO, 11 % K_2O, 9 % Na_2O, 3 % B_2O_3, and 0.9 % CdS was used, where SiO_2 serves as glass former, K_2O, Na_2O and B_2O_3 as flux to reduce the melting temperature, and ZnO as partner for CdS formation.

In preliminary glass making experiments the amount of S retained in the glass after melting was determined. This knowledge was needed to make a glass with a well-defined amount of S, and CdS nanoparticles as well. Also it was found that nanoparticles form faster for a melting time of the glass of 2.5 h as compared to 4 h. Related, the time needed to color the sample during the annealing process increased from 6 to 200 h for the melting time 2.5 and 4 h, respectively, indicating a decrease of the content of S and, therefore, the amount of CdS grown for elongated melting times.

Thus the glass batch used for the small angle scattering (SAS) was melted for 2.5 h in a recrystallized alumina crucible in an electrically heated shaftfurnace at 1400 °C. After this, the glass melt was quenched in air on a hot graphite plate and immediately annealed at 550 °C for 30 min. Subsequently, the samples were slowly cooled to room temperature to remove the stresses created by the quenching. By this procedure, a transparent, colorless bulk glass was synthesized.

Samples were then cut with a diamond wheel saw to dimension of 10×10×20 mm^3. Subsequent heat treatments initiated the growth of CdS crystals. Optical inspection has shown that annealing at 600 °C for different periods of time is best to produce a yellow color of the samples. After 6 h at this temperature the glass shows different tints from green-yellow to orange-yellow. Reference glass samples without CdS subjected to the same annealing remained colorless. After annealing the thickness of samples was reduced to 150 μm by cutting, grinding and final polishing with diamond suspension to achieve at least 13 % of X-ray transmission at 1.54 Å. This thickness meets also the neutron scattering conditions providing for a measured transmission of 70 % at 12 Å.

2.2 Experimental techniques

The samples were measured with a laboratory SAXS equipment in Juelich, Germany (BRUCKER NANOSTAR X-Ray Diffraction System, point collimation system, Cu Kα 1.54 Å, q-range between 0.005 and 0.3 [1/Å]) and with SANS using KWS-3 beamline at FRM II (focusing mirror system, neutron wavelength 12 Å, q-range between 0.0003 and 0.035 [1/Å]) in Garching, Germany. The data reduction involved correcting the radial integrated intensity profiles for transmission, thickness, detector efficiency and empty beam. The data were fitted with the program IRENA (IgorPro) which allows analyzing SAS data by immediate modeling of the scattering from several populations selecting forms and structure factors [35].

3. Results and discussion

Since the Guinier regime is outside the investigated window the amplitude of background scattering from the glass matrix is described by the scattering volume that is derived by the scattering intensity using basic SAS formula [35]:

$$I(q) = |\Delta\rho|^2 \int_0^\infty |F(q,r)|^2 V^2(r) NP(r) dr$$

where ρ is scattering length density, $\Delta\rho$ is contrast, *F(q,r)* is scattering form factor, *V(r)* is the particle volume, *N* is the total number of scattering particles, *P(r)* is the probability of occurrence of scatterers of size of *r*. If the chemical formula indicates that there are *k* types of atoms, of

which $\#_j$ are of variety *j* with scattering length $\langle b \rangle_j$, then the scattering length density ρ is given by [28]:

$$\rho = \frac{\rho_{bulk} N_A}{m} \sum_{j=1}^{k} \#_j \langle b \rangle_j$$

where $m = \sum \#_j m_j$ is the mass of the molecule, ρ_{bulk} is the bulk density, N_A is Avogadro constant. For X-ray scattering $\langle b \rangle_j = z_j r_e$, where z_j is atomic number, r_e is Thomson scattering length or classical electron radius. The calculated value of contrast between CdS phase and glass matrix used in modeling is $202 \cdot 10^{-12}$ A^{-4}.

Difference of curves in Fig. *1b* to *1d* with respect to an increase of scattering intensity for *q* above 0.02 $Å^{-1}$ with respect of annealing time arises from CdS nucleation and growth during the annealing. At this range the CdS response was not observed for the as-prepared glass (see Fig.1a) indicating an ionic state of Cd and S. All samples show pronounced scattering at *q* below 0.02 $Å^{-1}$ which we associate with large scale inhomogeneities due to density and concentration fluctuations which are common in multicomponent glasses [36-39]. It appears that this 'background' scattering evolves during the annealing. A more detailed assessment of this contribution will be published elsewhere.

At present, the emphasis is on a description of the formation of CdS nanoparticles. Thus, to describe the data we assume a system composed out of the glass matrix and CdS nanoparticles.

a)

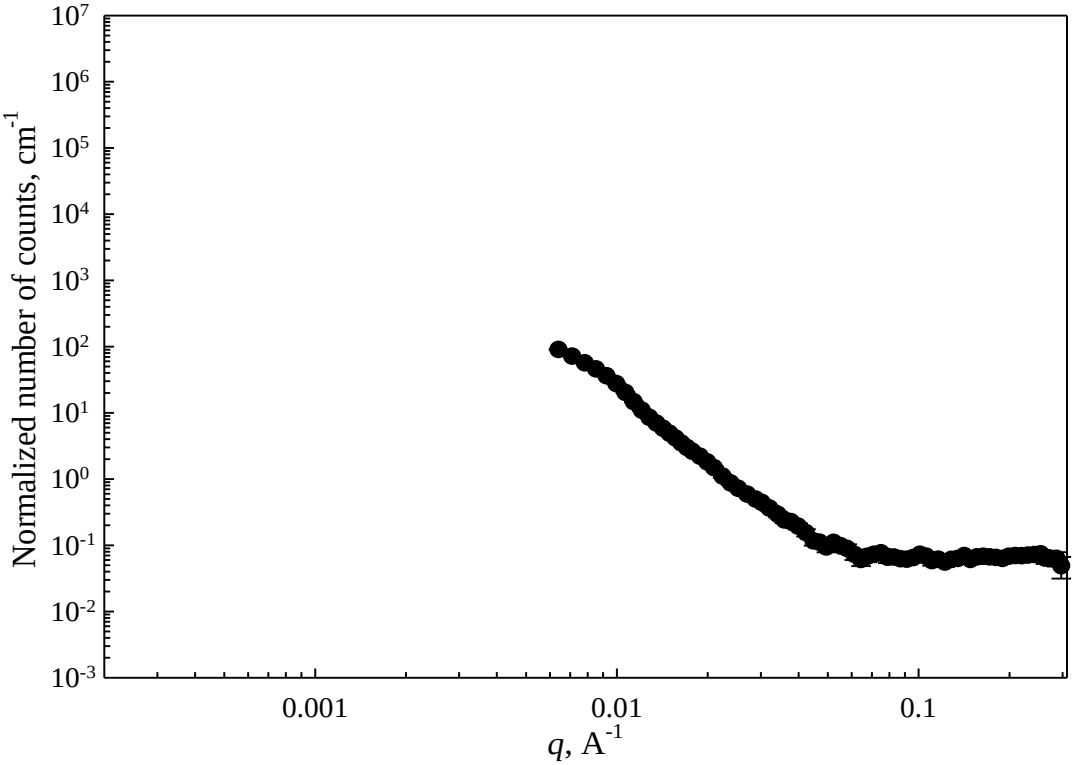
Normalized number of counts, cm-1
10^7
10^6
10^5
10^4
10^3
10^2
10^1
10^0
10^-1
10^-2
10^-3
0.001
0.01
0.1
q, A-1

b)

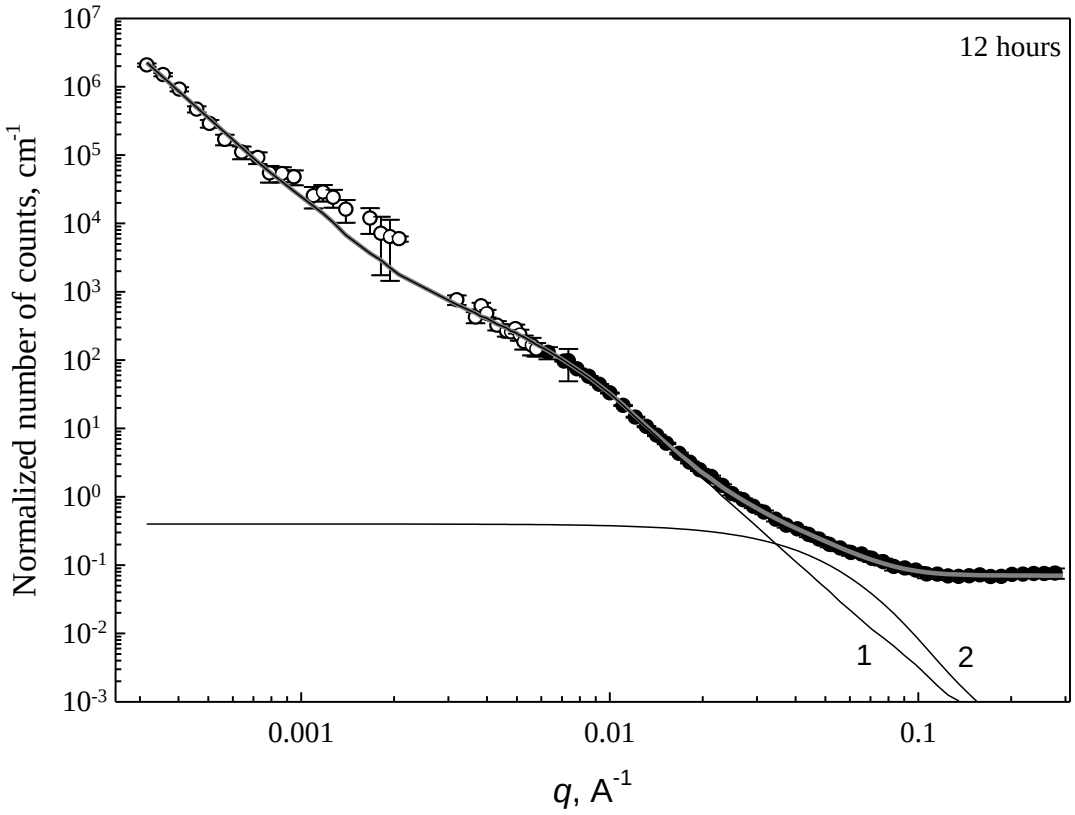
12 hours
Normalized number of counts, cm-1
10^7
10^6
10^5
10^4
10^3
10^2
10^1
10^0
10^-1
10^-2
10^-3
0.001
0.01
0.1
q, A-1
1
2

c)

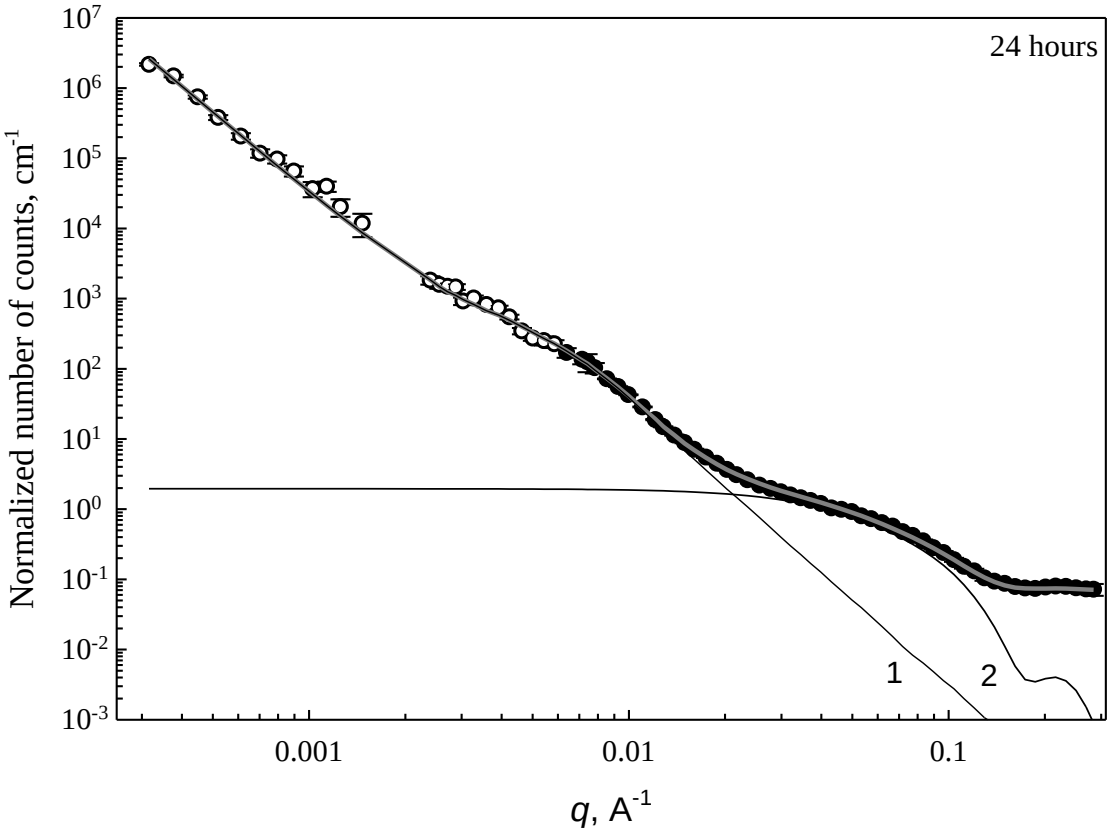
24 hours
Normalized number of counts, cm-1
10^7
10^6
10^5
10^4
10^3
10^2
10^1
10^0
10^-1
10^-2
10^-3
0.001
0.01
0.1
q, A-1
1
2

d)

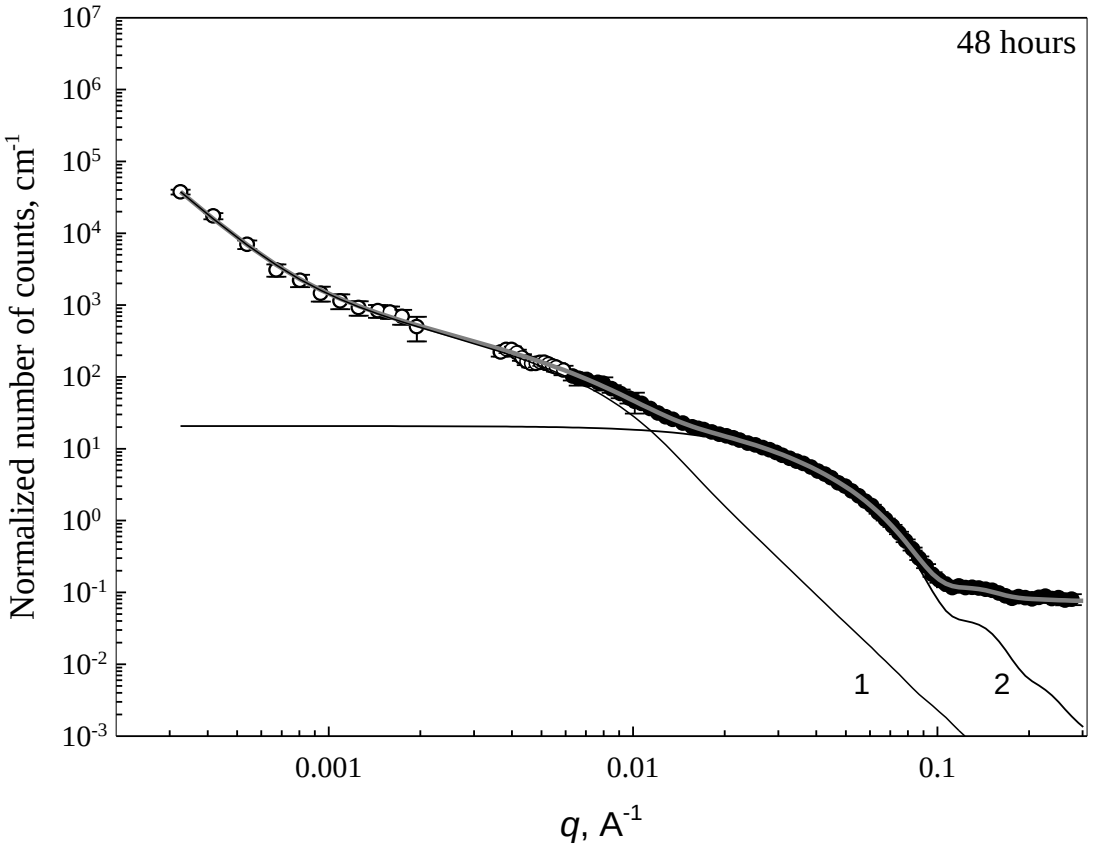

Fig. 1 Experimental SANS (open symbols) and SAXS (closed symbols) intensities (points with error bars) for samples as prepared (a) and annealed for 12 (*b*), 24 (*c*) and 48 (d) hours at 600 °C. Bold grey solid lines represent model curves composed out of glass background (1) and CdS particles (2) (see text for details).

The scattering signal from these fluctuations is modeled using two particle populations represented by a sphere with radius of about 17 000 Å (population 1) and a spheroid with a short and a long radius of about 250 and 17 000 Å, respectively, (population 2). The sum of these contributions is shown in Fig.1 as line 1. We note that these values which also vary with temperature in a range of 16 000÷17 000 and 200÷250 Å may not be related directly to the real physical extensions of the glass heterogeneities, but they are used to provide a description of the glass background.

The scattering intensity from the as-quenched Cd and S doped glass only shows the scattering from the glass matrix without CdS formation. This implies that the quenching procedure is efficient and suppresses the formation of nanoparticles.

The salient change in the SAS pattern is an increasing amplitude with annealing time for q values above 0.01 $Å^{-1}$, which reflects directly the formation of CdS particles. In particular, we

note that the experimental data develop well-defined oscillations at higher *q* values for annealing times of 24 h and for 48 h.

For the annealing time of 12 h the scattering can be described by a sphere with a radius of 34±4 Å. However, this approach proofs inadequate for longer annealing times and a description with a spheroid with an aspect ratio of 3 is needed. The size of the spheroid is increasing with time (see table 1). Further, the amount of precipitated CdS is increasing with time as evident from the graphs in Fig.1 and summarized in Table 1.

Table 1 –*Fitting parameters for the small angle scattering on CdS in silicate glass annealed at 600 °C for different periods of time.*

	Distribution Type	**Fitting Parameters**	**12 h**	**24 h**	**48 h**
		Shape	**Sphere**	**Spheroid short/long axis**	
Population 3	LogNormal	*Radius, Å*	34	24/72	40/120
		Standard Deviation, Å	4	2	2
		Total Volume CdS/glass, mm^3/cm^3	0.06	0.5	1

Analysis of the size of the CdS nanoparticles suggests that the annealing at 600 °C during the first 12 h period causes the nucleation of spherical CdS nanoparticles with a radius of about 34 Å. Prolonged heat treatment of 24 h and beyond leads to a change of the shape of the nanoparticle from spherical to spheroidal with an aspect ratio of 3 and reaching after 48 h a short and a long axis of 40 and 120 Å, respectively.

The volume increase between 12 and 24 h and between 24 and 48 h is about a factor of 8 and 2, respectively. Analysis of a single nanoparticle volume suspects that annealing from 12 to 24 h leads only to particle shape changing from sphere to spheroid with aspect ratio of 3 which is likely more energy preferable for a hexagonal structure of CdS nanoparticles. A width of lognormal distribution narrows substantially indicating the formation of nanoparticles with equal size and shape up to 24 h. Further annealing up to 48 h causes an increase of the single particle volume by a factor of 5 and an extension of the distribution width. This argues the transition from supersaturation to Ostwald ripening regime when CdS available is redistributed with negligible total volume changes. According to this mechanism the nanoparticles tend toward an isotropic growth forming particles with spherical shapes which are thermodynamically more stable because of the minimization of the overall surface energy. However, the experimental SAS results show anisotropic nanoparticle growth from sphere to spheroid. The analysis of size changes demonstrates that nanoparticles behave like clusters in colloidal solution which coarse

by attachment instead of a dissolution of smaller particles and ion re-precipitation as for Ostwald ripening. Nanoparticles after 24 h of annealing seem to be attached together with some sum surface changes due to time and temperature. This can be accounted for by oriented attachment, another growth mechanism in nanoscale systems where nanoparticles with common crystallographic orientations directly combine together leading the formation of nanoparticles with anisotropic shapes [40-44]. In this case the energy minimization can be attained by forming anisotropic particles, particularly in cases where growth occurs preferentially in the high energy planes [45].

4. Conclusions

In the present work CdS nanoparticles were grown isothermally in a glass matrix SiO_2-ZnO-K_2O-Na_2O-B_2O_3 with an annealing at 600 °C for different periods of time. The 2.5 h melting led to a sulfur content ten times less than initially introduced. Nevertheless this was sufficient for CdS nanoparticles to form and to be observed already by the appearance of a yellow color. The samples synthesized were studied here in more detail by small angle scattering. The combination of SANS and SAXS has shown the formation of CdS nanoparticles which size and shape changed with annealing time from spherical into spheroidal with the short and long radii up to 40 and 120 Å, respectively. Thus long annealing initiates formation of the nanoparticles with anisotropic shape of spheroid, exhibiting the particular character of crystal growth by the oriented attachments mechanism. In this case low diffusion in viscous matrix was overcome by time and high annealing temperature. Additionally it was found that the thermal treatment of the samples strongly influences on the nanoparticle size distribution that becomes narrower with longer annealing time up to 24 h. All the findings for glass nanotechnology can be used for the tuning of optical properties due to quantum size effects.

Acknowledgements

The authors thank W. Pyckhout-Hintzen for measurements and helpful discussions, and the BMBF of Germany (contract No. 05K10WEC) and RFBR (project No. 14-03-00869) for financial support.

References

[1] T. Vossmeyer, CdS nanoclusters: synthesis, characterization, size dependent oscillator strength, temperature shift of the excitonic transition energy, and reversible absorbance shift, J. Phys. Chem., 98 (1994) 7665-4673.

[2] J. M. Caruge, J. E. Halpert, V. Wood, V. Bulović, M. G. Bawendi, Colloidal quantum-dot light-emitting diodes with metal-oxide charge transport layers, Nature Photonics, 2 (2008) 247-250

[3] V. L. Colvin, M. C. Schlamp, A. P. Alivisatos, Light-emitting diodes made from cadmium selenide nanocrystals and a semiconducting polymer, Nature, 370 (1994) 354-357.

[4] S. Coe-Sullivan, W.-K. Woo, J. S. Steckel, M. Bawendi, V. Bulović, Tuning the performance of hybrid organic/inorganic quantum dot light-emitting devices, Organic Electronics, 4 (2003) 123-130.

[5] E. B. Stokes, A.D. Stiff-Roberta, C. T. Dameron, Quantum dots in semiconductor optoelectronic devices, The electrochemical society interface, (2006) 23-27.

[6] A.M. Glass, Materials for optical information processing**,** Science, 226 (1984) 657-662.

[7] A. Haesselbarth, A. Eychmuller, R. Eichberger, M. Giersig, A. Mews, H. Weller, Chemistry and photophysics of mixed cadmium sulfide/mercury sulfide colloids, J. Phys. Chem., 97 (1993) 5333-5340.

[8] A.P. Alivisatos, Semiconductor clusters, nanocrystals, and quantum dots, Science, 271 (1996) 933-937.

[9] M. Bruchez, M. Moronne, P Gin, S. Weiss, A.P. Alivisatos, Semiconductor nanocrystals as fluorescent biological labels, Science, 281 (1998) 2013-2016.

[10] Y. Wang, N. Herron, W. Mahler, Linear and nonlinear optical properties of semiconductor clusters, J. Opt. Soc. Am. B, 6 (1989) 808-813.

[11] Y. Medina-Gonzalez, W. Z. Xu, B. Chen, N. Farhanghi, P.A. Charpentier, CdS and CdTeS quantum dot decorated TiO_2 nanowires. Synthesis and photoefficiency, Nanotechnology, 22 (2011) 065603 (8pp)

[12] J. Zhao, J. A. Bardecker, A. M. Munro, M. S. Liu, Y. Niu, I-K. Ding, J. Luo, B. Chen, A. K.-Y. Jen, D. S. Ginger, Efficient CdSe/CdS quantum dot light-emitting diodes using a thermally polymerized hole transport layer, *Nano Lett.*, 6 (2006) 463-467.

[13] J. Kumar, A. Verma et al, Study of optical absorption and photoluminescence of quantum dots of CdS formed in borosilicate glass matrix, Phys. Scr., 79 (2009) 1-4.

[14] R. S. Sonawane, S.D. Naik, S.K. Apte, CdS/CdSSe quantum dots in glass matrix, Bull. Mater. Sci., 3 (2008) 495-499.

[15] H. Yukselici, P.D. Persans, T.M. Hayes, Optical studies of the growth of $Cd_{1-x}Zn_xS$ nanocrystals in borosilicate glass, Physical review, 52 (1995) 763-772.

[16] T.M. Hayes, L.B. Lurio et al, Order in CdS nanocrystals in glass, J. S.-st. comm., 117 (2001) 627-630.

[17] S.D. Naik, S.K. Apte, R. S. Sonawane, Nanostructured CdS/CdSSe glass composite for photonic application, J. of physics., 65 (2005) 707-712.

[18] J.D. Bryan, D.R. Gamelin, Doped semiconductor nanocrystals: synthesis, characterization, physical properties, and applications, J. Progress in inorganic chemistry, 54 (2005) 47-126.

[19] C. Liu, J. Heo, X. Zhang, J. L. Adam, Photoluminescence of PbS quantum dots embedded in glass, J. Non-Cryst. Solids, 354 (2008) 618-623.

[20] H. Okamoto, J. Matsuoka, H. Nasu, K. Kamiya, Effect of cadmium to sulfur ratio on the photoluminescence of CdS doped glasses, J. Appl. Phys., 75 (1994) 2251-2256.

[21] P. Nemec, P. Maly, Temperature study of trap related photoluminescence decay in CdS_xSe_{1-x} nanocrystals in glass, J. Appl. Phys. 87 (2000) 3342-3348.

[22] B. B. Kale, Confinement of nano CdS in designated glass: a novel functionality of quantum dot-glass nanosystems in solar hydrogen production, J. Mater. Chem., 17 (2007) 4297-4303.

[23] N.M. Pavlushkin, Chemical technology of the glass and glass ceramics, Moscow: Stroiizdat, 1983, p. 432. (in Russian)

[24] D.F. Eaton, Nonlinear optical materials, Science, 253 (1991) 281-287.

[25] A.M. Glass, Optical materials, Science, 235 (1987) 1003-1009.

[26] O. Glatter, O. Kratky, Small Angle X-ray Scattering, L. : Academic Press, 1982, 513 p.

[27] L.A. Feigin, D.I. Svergun, G.W. Taylor. Structure Analysis by Small -Angle X-ray and Neutron scattering, Plenum Press, New York., 1987, p.335.

[28] D.S. Sivia, Elementary Scattering Theory: For X-ray and Neutron Users, OUP Oxford, 2011. p. 216

[29] S. V. Gaponenko Optical properties of semiconductor nanocrystals, Cambridge University Press, 1998, 245 p.

[30] J. Kocík, J. Nebřeňský, I. Fanderlík. Barvení skla, SNTL, Praha 1978, s. 238

[31] I.M. Lifshitz, V.V. Slyozov, The kinetics of precipitation from supersaturated solid solutions, J. Phys. Chem. Solids, 19 (1961) 35-50.

[32] F.F. Abraham, Homogeneous nucleation theory, New York: Academic Press, 1974

[33] S.W. Koch, Dynamics of first order phase transitions in equilibrium and nonequilibrium systems, Berlin: Springer, 1984

[34] V.V. Slyozov, V.V Sagalovich, Diffusive decay of solid solutions, Sov. Phys. Uspekhi, 151 (1987) 67-106.

[35] J. Ilavsky, P. R. Jemian, Irena: tool suite for modeling and analysis of small-angle scattering, J. Appl. Cryst. 42(2) (2009) 347-353.

[36] A. Craievich, O. Alves, L. Barbosa, Formation and growth of semiconductor PbTe nanocrystals in a borosilicate glass matrix, J. Appl. Cryst. 30 (1997) 623-627.

[37] G. Walter, G. Goerigk, C. Rüssel, The structure of phosphate glass evidenced by small angle X-ray scattering, J. of Non-Cryst. Solids, 352 (2006) 4051–4061.

[38] L. Barbosa, V. Reynoso, A. de Paula, C. de Oliveira,O. Alves, A. Craievich, R. Marotti, C. Brito Cruz, C. Cesar, CdTe quantum dots by melt heat treatment in borosilicate glasses, J. of Non-Cryst. Solids, 219 (1997) 205–211.

[39] R. Le Parc, B. Champagnon, C. Levelut, V. Martinez, L. David, A. Faivre, I. Flammer, J. L. Hazemann, J. P. Simon, Density and concentration fluctuations in SiO2–GeO2 optical fiber glass investigated by small angle x-ray scattering, J. Appl. Phys. 103 (2008) 094917.

[40] R.L. Penn, J.F. Banfield, Imperfect Oriented Attachment: Dislocation Generation in Defect-Free Nanocrystals, J. F. Science, 281 (1998) 969-971.

[41] R.L. Penn, J.F. Banfield, Oriented attachment and growth, twinning, polytypism, and formation of metastable phases: insights from nanocrystalline TiO2. Am. Mineral., 83 (1998) 1077-1082.

[42] E. J. H. Lee, C. Ribeiro, E. Longo, E. R. Leite, Oriented Attachment: An Effective Mechanism in the Formation of Anisotropic Nanocrystals, J. Phys. Chem. B, 109 (2005) 20842-20846

[43] J. Zhang, Z. Lin, Y. Lan, G. Ren, D. Chen, F. Huang and M. Hong, A Multistep Oriented Attachment Kinetics: Coarsening of ZnS Nanoparticles in Concentrated NaOH, J. Am. Chem. Soc., 128 (2006) 12981-12987.

[44] J. Zhang, F. Huang, Z. Lin, Progress of nanocrystalline growth kinetics based on oriented attachment, Nanoscale, 2 (2010) 18–34.

[45] C. Ribeiro, C. Vila, J. E. Matos, J. Bettini, E. Longo, E. Leite, Role of the oriented attachment mechanism in the phase transformation of oxide nanocrystals, J. Chem.- Eur., 13 (2007) 5798-5803.